OPTIMAL LCL FILTER DESIGN FOR GRID-INTERFACED DISTRIBUTED POWER GENERATION SYSTEM

A Thesis submitted In Partial Fulfillment of the Requirements for the award of the degree of

Master of Technology
In
Power Electronics and Drives

By

DEEPIKA KUMARI

ROLL NO: 212EE4245

DEPARTMENT OF ELECTRICAL ENGINEERING

NATIONAL INSTITUTE TECHNOLOGY,

ROURKELA-769008

OPTIMAL LCL FILTER DESIGN FOR GRID-INTERFACED DISTRIBUTED POWER GENERATION SYSTEM

A Thesis to be submitted In Partial Fulfillment of the Requirements for the award of the degree of

Master of Technology
In
Power Electronics and Drives

By

DEEPIKA KUMARI

ROLL NO: 212EE4245

UNDER THE SUPERVISION OF

PROF. K.B. MOHANTY

DEPARTMENT OF ELECTRICAL ENGINEERING

NATIONAL INSTITUTE TECHNOLOGY,

ROURKELA-769008

Department Of Electrical Engineering
National Institute Technology,
Rourkela-769008

CERTIFICATE

This is to certify that the Thesis Report entitled "**Optimal LCL Filter Design For Grid-Interfaced Distributed Power Generation System**", submitted by **Ms Deepika Kumari** bearing **Roll No. 212EE4245** in partial fulfilment of the requirements for the award of Master of Technology in Electrical Engineering with specialization in "Power Electronics and Drives" during session 2012-2014 at National Institute of Technology, Rourkela is an authentic work carried out by her under my supervision and guidance.

I believe that the thesis fulfills part of the requirements for the award of degree of Master of Technology in Power Electronics and Drives. The results embodied in the thesis have not been submitted for award of any other degree.

Prof. K. B. MOHANTY
Dept. of Electrical Engineering
National Institute of Technology
Rourkela – 769008

Date:

Place: Rourkela

ACKNOWLEDGEMENTS

I would like to express my sincere gratitude to my supervisor **Prof. K. B. Mohanty** for his guidance, encouragement, and support throughout the course of this work. It was an invaluable learning experience for me to be one of his students. From him I have gained not only extensive knowledge, but also a sincere research attitude.

I express my gratitude to **Prof. A.K Panda,** Head of the Department, Electrical Engineering for his invaluable suggestions and constant encouragement all through the research work.

My thanks are extended to my colleagues in Power Control and Drives, who built an academic and friendly research environment that made my study at NIT Rourkela most memorable and fruitful.

I would also like to acknowledge the entire teaching and non-teaching staff of Electrical Department for establishing a working environment and for constructive discussions.

Finally, I am always indebted to all my family members, especially my parents, for their endless love and blessings.

DEEPIKA KUMARI

ROLL NO.:- 212EE4245

DECLARATION

I hereby declare that the research work carried out in the thesis has been carried out by me. The work is original and has not been submitted earlier as a whole or in part for a degree/diploma at this or any other institution / University.

Deepika Kumari
Roll. No. 212EE4245
Power Electronics and Drives
Department of Electrical Engineering

ABSTRACT

Optimal design of LCL filter for grid connected inverter system is studied. For that, initially normal design is considered. Higher order LCL filters are essential in meeting the interconnection standard requirement for grid-connected voltage source converters. The IEEE 1547-2008 specifications for high-frequency current ripple are used as a major constraint early in the design to ensure that all subsequent optimizations are still compliant with the standards.

The choice of switching frequency for pulse width modulation single-phase inverters, such as those used in grid-connected photovoltaic application, is usually a tradeoff between reducing the total harmonic distortion (THD) and reducing the switching loss. The total inductance per unit of the LCL filter is varied, and LCL parameter values which give the highest efficiency while simultaneously meeting the stringent standard requirements are identified. Then the conduction and switching losses that are caused by the filter are calculated and are optimized considering the level of reduction of harmonics. Hence the main aim of the study is to attenuate higher order harmonics along with the reduction in switching losses to ensure sinusoidal current injection into the grid. Further, the different switching schemes for single phase full bridge inverter are studied and compared to get the switching scheme which gives lesser switching losses.

The LCL filter is designed accordingly and optimal inductance and capacitance values are obtained. Novel small signal model of a three phase grid connected VSI has been derived and its relevant transfer functions have been deduced from it so as to analyze the system for designing a controller and also bode plots have been plotted. Stability Analysis of Grid-Connected Inverters with an LCL Filter Considering Grid Impedance and comparative study between unipolar and bi-polar switching scheme for grid-connected inverter system is also done. Simulation is done in MATLAB SIMULINK environment for feasibility of the study.

TABLE OF CONTENTS

LIST OF FIGURES

LIST OF TABLES

LIST OF SYMBOLS

V_{LN}	Line-to-neutral output voltage
u_i	Inverter output voltage
i_i	Inverter output current
u_g	Grid Voltage
i_g	Grid Current
f_{sw}	Switching Frequency
L_1	Inverter side inductance
L_2	Grid side inductance
ω_r	Resonant frequency
C_d	Damping Capacitor
R_d	Damping Resistor
$F_m(s)$	First order inertial element of the converter
$F_i(s)$	Transfer function of the current regulator
$Z_{gdq}(s)$	Grid-impedance matrix
$Y_{oc}(s)$	Output admittance matrix
$L_{dq}(S)$	Return-ratio matrix
Z_{dd}	Output impedance
f_o	Operating frequency

CHAPTER 1

INTRODUCTION

Overview

Research Motivation

Literature Review

Thesis Objectives

Organization of Thesis

1.1. OVERVIEW

Growing demand of power and limited availability of conventional sources are the two key issues worrying researchers to think other alternatives of generating power. That's why other non-conventional sources have become popular now-a-days. Simultaneously, rising cost and complexity in existing electricity distribution systems and the inability of current systems to serve remote areas reliably has led to search for alternate distribution methods. One viable solution is use of renewable energy sources directly at point of load, which is termed as Distributed Generation (DG).

Most renewable sources of energy, like wind, solar, fuel cell etc. are interfaced to the existing power supply by a power converter. This eliminates the transmission and distribution losses and improves reliability of the power supply. But use of power converters will also introduce undesirable harmonics that can affect nearby loads at the point of common coupling to the grid. Hence all such converters have a filter to eliminate these harmonics.

The present work is on design of such filters for high power (10's to 100's of kW),Pulse width modulated voltage source converters for grid-connected converter applications. The conventional method to interface these converters to grid is through a simple first order low-pass filter, which is bulky, inefficient and cannot meet regulatory requirements such as IEEE 512-1992 and IEEE 1547-2008. The design of efficient, compact higher order filters to attenuate the switching harmonics at the point of interconnection to the grid to meet the requirement of DG standards of interconnection is studied. Also different switching schemes for single phase unipolar full bridge inverter are studied and compared to get the switching scheme which gives lesser switching losses. The LCL filter is designed accordingly and optimal inductance and capacitance values are obtained. All the related models are simulated using the MATLAB software and graphs are studied.

1.2. RESEARCH MOTIVATION

In recent years availability of power in India has both increased and improved but demand has consistently outstripped supply and substantial energy and peak shortages prevailed in 2009-10. That's why non-conventional sources have become the center of attraction. Among these fast growing is the wind energy system. Now India has become fifth in installed capacity of wind power plant. As in 2012 the installed capacity of wind power in

India was 18,421 MW. But, as the wind is season and region based, it was not so reliable as long as Power Electronics had not been advanced much.

Now-a-days the interface of Power Electronics has made wind energy system one of the reliable sources. Most renewable sources of energy, like wind, solar, fuel cell etc. are interfaced to the existing power supply by a power converter this eliminates the transmission and distribution losses and improves reliability of the power supply. But use of power converters will also introduce undesirable harmonics that can affect nearby loads at the point of common coupling to the grid. Hence all such converters have a filter to eliminate these harmonics. An attempt is initiated to reduce harmonic content of Grid side converter in this project.

1.3. LITERATURE REVIEW

Energy crisis and the threatening increase of greenhouse gases have naturally caused more attention to the use of renewable energy resources in modem distribution networks. The dispersed nature of these resources, sometimes called Distributed Resources (DR), along with other technical and economical issues has consequently brought the subject of Distributed Generation (DG) into consideration [11].Many types of distributed resources produce electrical energy in the form of dc voltage source. Well known examples are photovoltaic (PV) and fuel cells.

Furthermore, in some other type of DR, although the generated electrical energy is in the form ac, it is preferred to perform energy exchange through an ac/dc/ac conversion stage for the incompatibility of the generated voltage and/or frequency with that of grid. Examples of this type are micro-turbines, in which the electrical energy is generated via high speed permanent magnet generators with the frequency around a few kilohertz, or in some types of wind turbines in which technical characteristics of the system do not allow direct connection of the generator to the utility grid [12].As a result, with currently available technologies, many DRs need a dc/ac conversion stage for energy transfer to the grid. Apparently, static dc/ac converters are the best alternative for this task and thus widely used in such applications.

Voltage Source Converters (VSC) is almost exclusively used for conversion of energy between a dc source and utility grid for the power range normally available in DR. The non-sinusoidal nature of PWM voltages at the output of these converters calls for adequate

filtering in order to limit the current harmonics injected to the grid. Traditionally, a simple first order L filter is used to connect converter to the grid and reduce injected harmonic currents. However, implementation of third-order LCL filters has been recently proposed by some researchers [13-15]. Despite many potential advantages, some important parameters must be carefully taken into consideration in design of an LCL filter. This subject, specifically when the converter is used to connect a DR to the utility grid for active power transfer, has not been rigorously studied and available literature on it is very limited. We are concerned with the investigation of LCL filters and their effects on the overall performance of a grid-connected VSC when the flow of power is from dc side to the ac utility grid. Analytical expressions and plots are provided for better understanding of the filter behavior.

1.4. THESIS OBJECTIVES

The objectives to be achieved in this study are:

- To construct the averaged small-signal model of the three-phase grid-connected three-level neutral-point-clamped inverter with a LCL filter.
- To calculate optimal value of inductance and capacitance of LCL filter.
- Relevant transfer functions have been deduced from model so as to analyse the system for designing a controller and also bode plots have been plotted.
- To calculate power loss in each individual filter component.
- Stability Analysis of Grid-Connected Inverters with an LCL Filter Considering Grid Impedance.
- Comparative study between unipolar and bi-polar switching scheme for grid-connected inverter system.
- To compare different switching schemes for single phase unipolar full bridge inverter.

1.5. ORGANIZATION OF THESIS

This thesis consists of introductory chapter and four other chapters arranged as follows:

Chapter 2 covers the various filter topologies .Optimal design of filter along with conduction losses are discussed.

Chapter 3 presents the detailed study of Small Signal Modeling of Three-Phase Grid Connected Inverter System. D Channel Small-Signal Circuit is constructed for the study of stability. Stability Margin of a Grid-Connected Inverter Controlled with the Converter-Side Current is also discussed in the end.

Chapter 4 concerns about Comparative Study between Unipolar and Bipolar Switching Scheme with LCL Filter of Grid Connected Inverter System. Switching Losses of Inverter and Harmonics are also discussed in this chapter.

Chapter 5 provides the simulation results and discussion on the graphs so obtained.

Chapter 6 summarizes the thesis with a general conclusion and scope for future work followed by references.

CHAPTER 2

FILTER DESIGN AND CALCULATION OF LOSSES

Introduction

Filter Topologies

Design of the LCL Filter

Power Losses

Total Loss in the LCL Filter

Summary

2.1. INTRODUCTION

Optimal design of LCL filter for grid interfaced distributed power generation system is studied. For that, initially normal design is considered. Higher request LCL channels are crucial in gathering the interconnection standard necessity. The IEEE 1547-2008 determinations for high-frequency current ripple are utilized as a real imperative ahead of schedule in the outline to guarantee that all resulting improvements are still agreeable with the models.

2.2. FILTER TOPOLOGIES

The output filter helps in reducing the harmonics in generated current caused by semiconductor device switching. There are various types of filters. The simplest one is the filter inductor connected to the inverter's output. But various combinations of inductor and capacitors like LC or LCL can be used. The schematic diagram of a single phase grid connected inverter along with LCL filter is shown in Fig. 2.1.

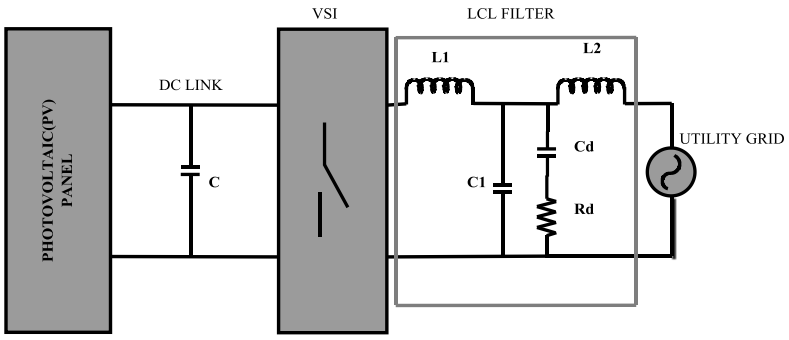

Fig. 2.1. Single Phase Grid Connected Inverter along with LCL Filter

1. L-Filter

The L-Filter is the first order filter with attenuation 20dB/decade over the entire frequency range. Hence this type of filter is suitable for converters with high switching frequency, where the attenuation is sufficient. On the other side, inductance greatly decreases dynamics of the whole system converter filter [2].

2. LC-Filter

The LC-Filter is the second order filter having better damping as compared to L-Filter. It is easy to design and works mostly without problems. This filter provides 12dB per

octave of attenuation after the cut-off frequency f_o, it has no gain before f_o, but it presents a peaking at the resonant frequency f_o. Transfer function of the LC-filter is

$$F(s) = \frac{1}{1+s\,L_F+s^2 L_F\,C_F} \qquad (2.1)$$

In order to suppress the negative behaviour near cut-off frequency the damping circuit is added to the filter. The damping can be either series or parallel. The damping circuit selection influences the transfer function of the filter.

3. LCL- Filter

The LCL-filter is a third order filter having attenuation of 60db/decade for frequencies above full resonant frequency, hence lower switching frequency for the converter switches could be utilized . Decoupling between the filter and the grid connected inverter having grid side impedance is better for this situation and lower current ripple over the grid inductor might be attained. The LCL filter will be vulnerable to oscillations too and it will magnify frequencies around its cut-off frequency. Therefore the filter is added with damping to reduce the effect of resonance. Therefore LCL-filter fits to our application. In the interim, the aggregate inductance of the received LCL filter is much more diminutive as contrasted with the L filter. Commonly, the expense is lessened. Besides, enhanced dynamic execution, harmonic attenuation and decreased volume might be accomplished with the utilization of LCL filter. The conduction and switching losses that are caused by the filter are calculated and are optimized considering the level of reduction of harmonics.

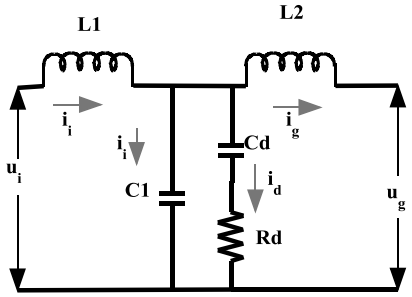

Fig. 2.2. Single Phase Equivalent Circuit of an LCL Filter with Passive Damping

2.3. DESIGN OF THE LCL FILTER

The greater part of the configuration mathematical statements are communicated in per unit basis of the volt-ampere rating of the power converter. Single phase equivalent circuit of the LCL filter with passive damping is demonstrated in Fig.2.2. The line-to-neutral

output voltage V_{LN} is the base voltage, and the three-phase kilovolt-ampere rating is the base volt-ampere.The fundamental frequency of 50 Hz is the base frequency. The inverter yield voltage and current are spoken to by u_i and i_i, and the output voltage and current are spoken to by u_g and i_g. The switching frequency is spoken to by f_{sw} (in hertz) or ω_{sw} (in radians for every second). We are considering power grid as a perfect voltage source, i.e., zero impedance, and it is supplying a steady voltage/current just at the fundamental frequency[1].The LCL filter transfer function which influences the closed-loop system bandwidth in the grid-connected mode of operation is represented as:

$$F(s) = \frac{1}{s\,(L_1+L_2)+s^3 L_1 L_2\,C} \tag{2.2}$$

$$\omega_r = \frac{1}{L_p\,C} \tag{2.3}$$

$$L_P = \frac{L_1 \times L_2}{L_1 + L_2} \tag{2.4}$$

$$L_1 = a_L L_2 \tag{2.5}$$

$$\omega_r = \frac{1}{L_p \frac{a_L}{(a_L+1)^2} \times C} \tag{2.6}$$

Where, L_1 :- Inverter side inductance & L_2 :- Grid side inductance.

Taking resonant frequency ω_r constant, is derived at the minimum capacitance as follows,

$$\frac{\delta C}{\delta a_L} = 0 \tag{2.7}$$

Whose simplification gives a_L=1. . In this way, the most modest capacitance estimation of the LCL filte is gotten when L_1=L_2. Equation (2.3) becomes

$$\omega_r{}^2 = \frac{4}{L\,C} \tag{2.8}$$

After solving equation (2.2) and (2.4).We get.

$$L = \frac{1}{\omega_{SW}\left|\frac{i_g}{u_i}\right|\left|1-\frac{\omega_{SW}{}^2}{\omega_r{}^2}\right|} \tag{2.9}$$

It gives the base $L=L_1+L_2$ per unit that will fulfill the standard suggestions for current ripple at the obliged switching frequency.

Passive Damping Scheme

The real target of damping is to decrease the Q-element at the resonance frequency without influencing the frequency response at different frequencies. The aggregate power dispersal in the damping circuit is additionally an imperative parameter to be considered.

$L_1 = L_1$

$C_d = a_C C_1$ and $C = C_1 + C_d$ (2.10)

Where, C_d is the damping capacitor.

The required transfer function is

$$\frac{u_c(j\omega)}{u_i(j\omega)} = \frac{0.5+j0.5\omega C_d R_d}{\left(1-\frac{\omega_{SW}{}^2}{\omega_r{}^2}\right)+j\omega R_d\left(1-\frac{\omega_{SW}{}^2}{\omega_r{}^2}\ \frac{1}{1+a_C}\right)} \quad (2.11)$$

$$Q_C = \left|\frac{1+j\omega_r R_d(\frac{a_C}{1+a_C})}{j\omega_r R_d(\frac{a_C}{1+a_C})^2}\right| \quad (2.12)$$

$$R_d = \sqrt{\frac{L}{C}} \quad (2.13)$$

Where, R_d is the damping resistor.

2.4. POWER LOSSES

Power losses are calculated at fundamental frequency and switching frequency.

1) Inductor: Essentially, losses in inductor are separated into core and copper loss. In spite of the fact that, there are some extra losses which are unimportant. So with the assistance of Magnetic design software both core and copper losses at switching and fundamental frequencies are ascertained. [3].

2) Damping Circuit and Capacitor:

Fundamental Frequency Power Loss

At fundamental frequency (50 Hz), the grid voltage is same as that of the voltage across the damping circuit (u_c) [4]. Therefore, $u_c = u_g$

$$P_{d(50)} = \frac{u_c{}^2 \omega_{50}{}^2 C_d{}^2 R_d}{1+\omega_{50}{}^2 C_d{}^2 R_d{}^2} \quad (2.12)$$

Switching Frequency Power Loss

At the switching frequency Grid is considered as a short circuited. However it is an ideal voltage source at fundamental frequency (50 Hz). So at switching frequency u_g=0.Switching frequency power loss can be represented as:

$$P_{d(sw)} = \frac{{u_i}^2 \omega_{sw} C_d}{1+{\omega_{sw}}^2 {C_d}^2 {R_d}^2} \frac{a^2+b^2}{c^2+d^2} x \quad (2.13)$$

$x = \omega_{sw} C_d R_d$

2.5. TOTAL LOSS IN THE LCL FILTER

Complete losses incorporates core and copper loss both of every single part of filter. We can ascertain the base L_{pu} and C_{pu} that is obliged to meet the determinations of current harmonics for the converter appraisals defined in Table 2.1.

TABLE 2.1
CONVERTER RATINGS USED FOR CALCULATIONS

KVA	V_{base}	I_{base}	f_1	f_{sw}	f_r	V_{dc}
Kva	V	A	Hz	kHz	KHz	V
10	239.6	13.91	50	10	1	861

Communicating all qualities in per unit of the base rating detailed by Table 2.1 and utilizing mathematical equation (2.5)

L_{pu} =0.015 & C_{pu}=0.661

2.6. SUMMARY

In this section we talked about how LCL filter is superior to L and LC filter. Ideal estimation of inductance and capacitance of LCL channel is ascertained. LCL parameter values which give the most astounding effectiveness are recognized by fluctuating the aggregate inductance for every unit of the LCL filter, while at the same time meeting the stringent standard necessities. Then the conduction and switching losses that are caused by the filter are calculated and are optimized considering the level of reduction of harmonics. Hence the main aim of the study is to attenuate higher order harmonics along with the reduction in switching losses to ensure sinusoidal current injection into the grid.

CHAPTER 3

MODELING

Introduction

Small Signal Modeling Of Three-Phase Grid Connected Inverter System

D Channel Small-Signal Circuit

Stability Analysis of the Grid-Connected Inverter

Stability Analysis of a Grid-Connected Inverter Having Converter-Side Current Control

Summary

3.1. INTRODUCTION

Novel small signal model of a three phase grid connected VSI has been derived and its relevant transfer functions have been deduced from it so as to analyze the system for designing a controller and also bode plots have been plotted. The averaged small-signal equations are expressed in state space representation which helps in analysis of stability of the overall system.

3.2. SMALL SIGNAL MODELING OF THREE-PHASE GRID CONNECTED INVERTER SYSTEM

To derive the averaged small-signal model, there are the processes composed of averaging, perturbing and linearizing step about the circuit equations [6]. Fig. 3 is the circuit schematic of 3P-GC-3L-NPC inverter system with a LCL filter. The circuit equation is derived as follows:

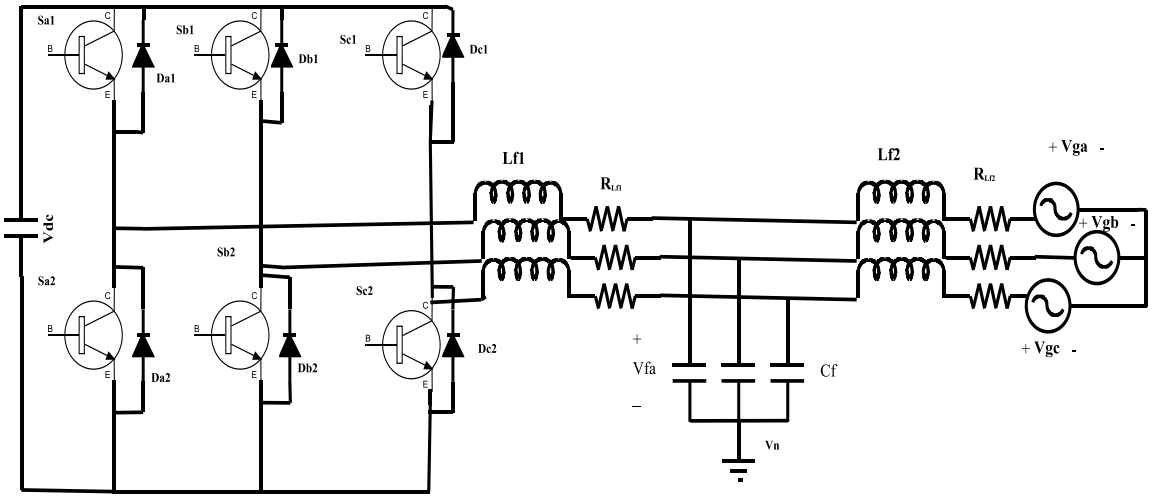

Fig. 3.1. Grid-connected three-level NPC inverter with a LCL filter.

$$v_{ph} = L_{f1}\frac{di_{sph}}{dt} + R_{L_{f1}} i_{sph} + v_{fph} + v_N$$

$$v_{fph} + v_N = L_{f2}\frac{di\_gph}{dt} + R_{L_{f2}} i_{gph} + v_{gph} \quad (3.1)$$

$$C_f \frac{di_{fph}}{dt} = i_{sph} - i_{gph} \quad (3.2)$$

Averaged Model and DQ-Coordinate Transformation

$$\frac{d\bar{\imath}_{sdq}}{dt} = -\frac{R_{Lf1}}{L_{f1}}\bar{\imath}_{sdq} - \frac{1}{L_{f1}}\bar{v}_{fdq} + \frac{1}{L_{f1}}(d_{pdq} - d_{ndq})\bar{v}_{dc} - \begin{bmatrix} 0 & -\omega \\ \omega & 0 \end{bmatrix}\bar{\imath}_{sdq} \quad (3.3)$$

$$\frac{d\bar{\imath}_{gdq}}{dt} = -\frac{R_{Lf2}}{L_{f2}}\bar{\imath}_{gdq} - \frac{1}{L_{f2}}\bar{v}_{fdq} - \begin{bmatrix} 0 & -\omega \\ \omega & 0 \end{bmatrix}\bar{\imath}_{gdq} \quad (3.4)$$

$$\frac{d\bar{v}_{fdq}}{dt} = \frac{1}{C_f}\bar{\imath}_{sdq} - \frac{1}{C_f}\bar{\imath}_{gdq} - \begin{bmatrix} 0 & -\omega \\ \omega & 0 \end{bmatrix}\bar{v}_{fdq} \quad (3.5)$$

Perturbed and Linearized Model

The perturbed values added to the small-signal ac variation (ˆ) around the operating dc point. After the linearization step neglecting nonlinear high-order ac terms, the averaged small-signal equations are obtained as:

$$\frac{d\hat{\imath}_{sdq}}{dt} = -\frac{R_{Lf1}}{L_{f1}}\hat{\imath}_{sdq} - \frac{1}{L_{f1}}\hat{v}_{fdq} + \frac{1}{L_{f1}}(\hat{d}_{pdq} - \hat{d}_{ndq})V_{dc} - \begin{bmatrix} 0 & -\omega \\ \omega & 0 \end{bmatrix}\hat{\imath}_{sdq}$$

$$+\frac{1}{L_{f1}}(D_{pdq} - D_{ndq})\hat{v}_{dc} \quad (3.6)$$

$$\frac{d\hat{\imath}_{gdq}}{dt} = -\frac{R_{Lf2}}{L_{f2}}\hat{\imath}_{gdq} - \frac{1}{L_{f2}}\hat{v}_{gdq} + \frac{1}{L_{f2}}\hat{v}_{fdq} - \begin{bmatrix} 0 & -\omega \\ \omega & 0 \end{bmatrix}\hat{\imath}_{gdq} \quad (3.7)$$

$$\frac{d\hat{v}_{fdq}}{dt} = \frac{1}{C_f}\hat{\imath}_{sdq} - \frac{1}{C_f}\hat{\imath}_{gdq} - \begin{bmatrix} 0 & -\omega \\ \omega & 0 \end{bmatrix}\hat{v}_{fdq} \quad (3.8)$$

For the control of the grid current, a novel control terms are defined as follows

$$\hat{d}_{md} = \hat{d}_{pd} - \hat{d}_{nd} \quad (3.9)$$

$$\hat{d}_{mq} = \hat{d}_{pq} - \hat{d}_{nq} \quad (3.10)$$

With the novel control terms, the averaged small-signal equations are obtained as:

$$\frac{d\hat{\imath}_{sdq}}{dt} = -\frac{R_{Lf1}}{L_{f1}}\hat{\imath}_{sdq} - \frac{1}{L_{f1}}\hat{v}_{fdq} + \frac{1}{L_{f1}}\hat{d}_{mdq}V_{dc} - \begin{bmatrix} 0 & -\omega \\ \omega & 0 \end{bmatrix}\hat{\imath}_{sdq} + \frac{1}{L_{f1}}D_{mdq}\hat{v}_{dc} \quad (3.11)$$

$$\frac{d\hat{\imath}_{gdq}}{dt} = -\frac{R_{Lf2}}{L_{f2}}\hat{\imath}_{gdq} - \frac{1}{L_{f2}}\hat{v}_{gdq} + \frac{1}{L_{f2}}\hat{v}_{fdq} - \begin{bmatrix} 0 & -\omega \\ \omega & 0 \end{bmatrix}\hat{\imath}_{gdq} \quad (3.12)$$

$$\frac{d\hat{v}_{fdq}}{dt} = \frac{1}{C_f}\hat{\imath}_{sdq} - \frac{1}{C_f}\hat{\imath}_{gdq} - \begin{bmatrix} 0 & -\omega \\ \omega & 0 \end{bmatrix}\hat{v}_{fdq} \quad (3.13)$$

The averaged small-signal equations can be expressed by state space representation is given as

$$\dot{\boldsymbol{x}} = \boldsymbol{Ax} + \boldsymbol{Bu} \tag{3.14}$$

$$\dot{\boldsymbol{x}} = [\,\hat{\imath}_{sd}\ \hat{\imath}_{sq}\ \hat{\imath}_{gd}\ \hat{\imath}_{gq}\ \hat{v}_{fd}\ \hat{v}_{fq}]^{\boldsymbol{T}} \tag{3.15}$$

$$\boldsymbol{u} = [\,\hat{v}_{dc}\ \hat{d}_{md}\ \hat{d}_{mq}\ \hat{v}_{gd}\ \hat{v}_{gq}]^{\boldsymbol{T}} \tag{3.16}$$

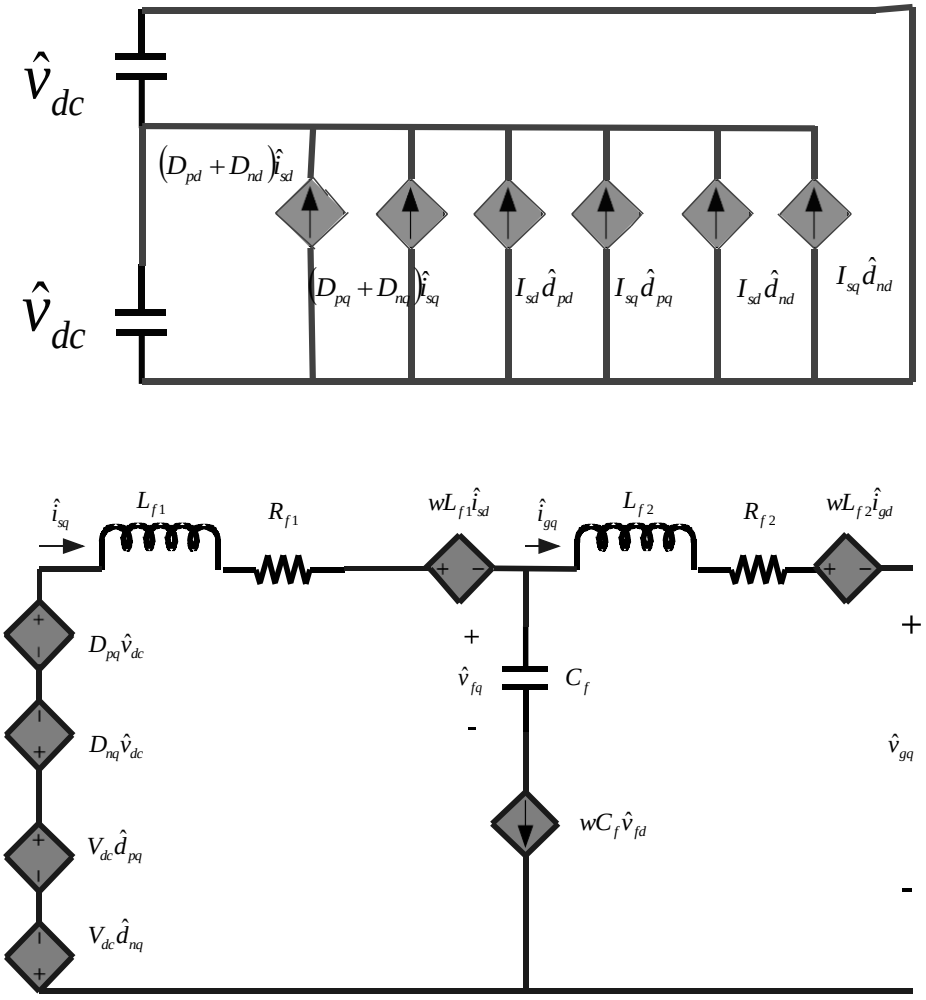

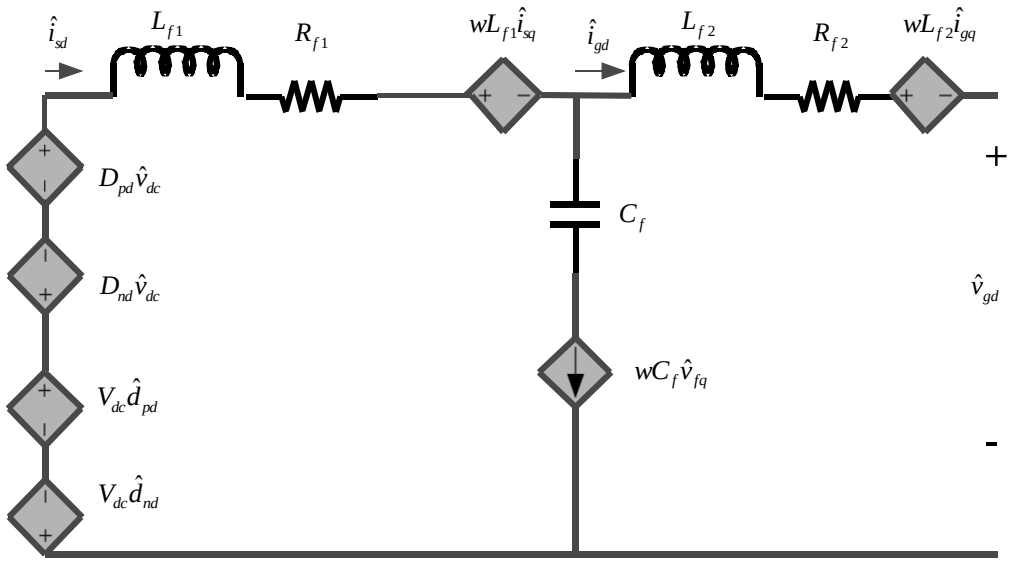

Fig. 3.2. Grid-connected three-level NPC inverter with a LCL filter

$$\boldsymbol{A} = \begin{bmatrix} -\frac{R_{Lf1}}{L_{f1}} & \omega & 0 & 0 & -\frac{1}{L_{f1}} & 0 \\ -\omega & \frac{-R_{Lf1}}{L_{f1}} & 0 & 0 & 0 & -\frac{1}{L_{f1}} \\ 0 & 0 & -\frac{R_{Lf2}}{L_{f2}} & \omega & -\frac{1}{L_{f2}} & 0 \\ 0 & 0 & -\omega & -\frac{R_{Lf2}}{L_{f2}} & 0 & \frac{1}{L_{f2}} \\ \frac{1}{C_f} & 0 & -\frac{1}{C_f} & 0 & 0 & \omega \\ 0 & \frac{1}{C_f} & 0 & -\frac{1}{C_f} & -\omega & 0 \end{bmatrix} \tag{3.17}$$

$$\boldsymbol{B} = \begin{bmatrix} \frac{D_{md}}{L_{f1}} & \frac{V_{dc}}{L_{f1}} & 0 & 0 & 0 \\ \frac{D_{md}}{L_{f1}} & 0 & \frac{V_{dc}}{L_{f1}} & 0 & 0 \\ 0 & 0 & 0 & -\frac{1}{L_{f2}} & 0 \\ 0 & 0 & 0 & 0 & -\frac{1}{L_{f2}} \\ 0 & 0 & 0 & 0 & 0 \end{bmatrix} \tag{3.18}$$

3.3. D CHANNEL SMALL-SIGNAL CIRCUIT

In order to determine the d-d channel output impedance of the grid-connected inverter, the coupling terms in Fig. 3.2 are neglected. The d channel small-signal circuit is shown as Fig. 3.3. R_1 and R_2 are neglected because of their small values. As per the small-signal circuit

shown in Fig. 3.3, the transfer function from the duty cycle d to the converter-side current i_{1d} is described as follows

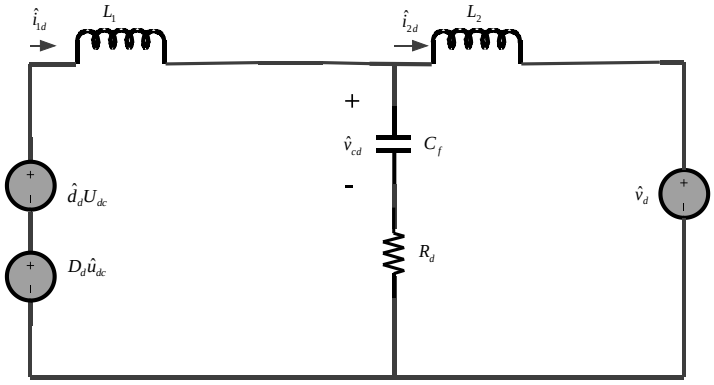

Fig 3.3. D channel small-signal circuit.

$$G_{id1}(s) = \frac{U_{dc}(s^2 C_f L_2 + sC_f R_d + 1)}{s^3 C_f L_1 L_2 + s^2 C_f R_d (L_1 + L_2) + s(L_1 + L_2)} \tag{3.19}$$

The transfer function from the duty cycle d to the grid-side current i_{2d} is described as follows:

$$G_{id2}(s) = \frac{U_{dc}(sC_f R_d + 1)}{s^3 C_f L_1 L_2 + s^2 C_f R_d (L_1 + L_2) + s(L_1 + L_2)} \tag{3.20}$$

For passive damping:

The transfer function from the duty cycle d to the grid-side current i_{2d} is described as follows:

$$G_{id2}(s) = \frac{U_{dc}(sCR_d + 1)}{s^4 L_1 L_2 C_f C R_d + s^3 (C_f + C) L_1 L_2 + s^2 C R_d (L_1 + L_2) + s(L_1 + L_2)} \tag{3.21}$$

The d-d channel open-loop output impedance is described as follows:

$$z_{00}(s) = \frac{s^3 C_f L_1 L_2 + s^2 C_f R_d (L_1 + L_2) + s(L_1 + L_2)}{(s^3 C_f L_1 + sC_f R_d + 1)} \tag{3.22}$$

The closed-loop d-d channel output impedance of the grid-connected inverter with the converter current control is shown as follows:

$$z_{dd_1}(s) = \frac{(s^2 C_f L_2 + sC_f R_d + 1)}{\frac{(sC_f R_d + 1)^2}{\Delta(s)(1 + T_{m1}(s))} + sC_f} \tag{3.23}$$

where,

$\Delta(s) = s^3 C_f L_1 L_2 + s^2 C_f R_d (L_1 + L_2) + s(L_1 + L_2)$

$T_{m1} = G_{id1}(s) F_i(s) F_m(s)$

$F_m(s)$ is the first order inertial element of the converter.

$F_i(s)$ is the transfer function of the current regulator.

3.4. STABILITY ANALYSIS OF THE GRID-CONNECTED INVERTER

The grid side current of the grid-connected inverter is communicated as:

$$I_{2dq}(s) = \left(I + Z_{gdq}(s) Y_{oc}(s)\right)^{-1} \left(I_{dq} - Y_{oc}(s) E_{dq}(s)\right) \quad (3.24)$$

Under the condition of an ideal grid, the inverter is assumed to work well and steadily. According to the above equation, when cascading the high-impedance grid, the system is stable if the return-ratio matrix $Z_{gdq}(s) Y_{oc}(s)$ satisfies the generalized Nyquist stability criterion and a sufficient stability margin is guaranteed [7].

Since return- ratio matrix is the second order matrix, it consist of two eigenvalues $l_1(s)$ and $l_2(s)$. According to the generalized Nyquist stability criterion, the grid-connected system is stable if and only if the net sum of the anticlockwise encirclements of the critical point (-1, j0) by the set of characteristic loci of $L_{dq}(S)$ is equal to the total number of right-half plane poles for the grid-impedance matrix $Z_{gdq}(s)$ and the output admittance matrix $Y_{oc}(s)$ of the grid-connected inverter.0 The eigenvalues of the return-ratio matrix $L_{dq}(S)$ are derived as follows:

$$l_1(s) = \left(sL_g + R_g + j\omega L_g\right) Y_{dd}(s) \quad (3.25)$$

$$l_2(s) = \left(sL_g + R_g - j\omega L_g\right) Y_{dd}(s) \quad (3.26)$$

The inductance L_g and the resistance R_g in the grid impedance are assumed to be 1mH and 1Ω, respectively.

3.5. STABILITY ANALYSIS OF A GRID-CONNECTED INVERTER HAVING CONVERTER-SIDE CURRENT CONTROL

When the system is controlled with the grid-side current, the grid-connected system does not satisfy the generalized Nyquist stability criterion. In this area we will principally investigates the stability margin of a grid associated inverter controlled with the converter-side current.

As for closed-loop control system, a certain stability margin should be required in addition to satisfying the generalized Nyquist stability criterion. Generally, in order to guarantee sufficient stability of the grid-connected system, that phase margin PM >60 ^{0} and gain margin GM > 6dB should be satisfied. The d-d channel output impedance of the inverter is related to the LCL-filter parameters, the switch frequency, the DC-side voltage and the current-loop regulation parameters. The impact of the LCL-filter parameters on the stability margin of the grid associated system is likewise mulled over. As the converter-side inductance L_1 has little influence on the output impedanceZ_{dd}.

According to eqn. 3.25 and eqn. 3.26 ,the magnitude of the eigenvalue $l_1(s)$ is always less than $l_2(s)$ and the Nyquist plot for the eigenvalue $l_2(s)$ is surrounded by $l_1(s)$, then the stability margin of the grid-connected system can be studied based on the eigenvalue $l_1(s)$ of the return-ratio matrix $L_{dq}(s)$. In order to analyze the influence of the resistive component in the grid impedance on the stability margin $l(s)$ is introduced as:

$$l(s) = \left(sL_g + j\omega L_g\right)Y_{dd}(s) \tag{3.27}$$

The resistive component in the grid impedance is able to improve the stability margin of the grid-connected system. In order to guarantee a sufficient stability margin for the system, this paper considers extreme cases and $l(s)$ is utilized to analyze the stability margin of system. Therefore, the steadiness examination of a grid connected system with an LCL filter is changed over into a study of the d-d channel yield impedance $Z_{dd}(s)$and the inductive segment $Z_{Lg}(s)$ in the grid impedance.

Neglecting the high-order term $\frac{\left(sC_fR_d+1\right)^2}{\Delta(s)(1+T_{m1}(s)}$, the output impedance Z_{dd}(s) is approximated as:

$$z_{dd_1}(s) = \frac{(s^2C_fL_2+sC_fR_d+1}{\frac{\left(sC_fR_d+1\right)^2}{\Delta(s)(1+T_{m1}(s)}+sC_f} \approx sL_2 + \frac{1}{sC_f} + R_d \qquad (3.28)$$

From (3.28), it is observed that the simplified d-d channel output impedance Z_{dd}(s) can be regarded as a series connection of the grid-side inductance and the capacitor branch.

3.6. SUMMARY

In this chapter, the averaged small-signal model is derived, which is composed of processes like averaging, perturbing and linearizing step about the circuit equations. The d-d channel output impedance of the grid associated inverter is acquired. Steadiness Analysis of Inverters with a LCL Filter mulling over Grid Impedance is carried out. Stability margin of an inverter controlled with the converter-side current is contemplated in this part.

CHAPTER 4

SWITCHING SCHEME

Introduction

Relative Study between Unipolar and Bipolar Switching Scheme with LCL Filter

Switching Losses of Inverter

Harmonics

Summary

4.1. INTRODUCTION

Unipolar switching scheme of the inverter with LCL channel can generally diminish the inverter current ripple to infuse sinusoidal current into the grid as contrasted with the bipolar switching scheme of inverter. Further, the different switching schemes for single phase full bridge inverter are studied and compared to get the switching scheme which gives lesser switching losses. Harmonic analysis is also done for L and LCL filter.

4.2. RELATIVE STUDY BETWEEN UNIPOLAR AND BIPOLAR SWITCHING SCHEME WITH LCL FILTER

Ripple Current Calculation

When the switching frequency $f_{sw} > f_o$(operating frequency) , then the inverter output is regarded to be constant during the switching intervals T_S[8].

For unipolar PWM inverter .the filter inductor current [9]:

$$\Delta i_{pk-pk}(wt) = \frac{T_S V_{dc}}{2L}(1 - m_a \sin\omega t).m_a \sin\omega t \quad (4.1)$$

For bipolar PWM inverter, the filter inductor current:

$$\Delta i_{pk-pk}(wt) = \frac{T_S V_{dc}}{4L}(1 - {m_a}^2 \sin^2\omega t) \quad (4.2)$$

where V_{dc} can be replaced by $V_{dc}/2$.

TABLE 4.1
DESIGN PARAMETERS

PARAMETERS	VALUE
Rated Power P	1 kVA
Rated Voltage V	230 V
Operating Frequency f_o	50 Hz
Switching Frequency f_{sw}	5 KHz

TABLE 4.2

FILTER VALUES AND THD% FOR UNIPOLAR SWITCHING SCEHME

Filter	L	LC	LCL
Inductance	1.475 mH	1.475 mH	L_1=1.028mH L_2=0.4469 mH
Capacitance		16.44μH	16.44μ F
Resistance			3.15Ω
THD%	5.95	1.58	0.7

TABLE 4.3

FILTER INDUCTANCE VALUE AND THD% FOR BI-POLAR SWITCHING SCHEME

	L	LC	LCL
Inductance	0.405 mH	0.405 mH	L_1=0.2833 mH L_2=0.1232 mH
Capacitance		16.44 μH	16.44 μH
Resistance			1.65 Ω
THD%	6.08	2.7	1.5

The result in the above table shows that the unipolar switching scheme can to a great extent decrease the inverter current ripple to infuse sinusoidal current into the grid as contrasted with the bipolar switching scheme of inverter with LCL filter. Further, it give great grid synchronization without information of grid impedance.

4.3. SWITCHING LOSSES OF INVERTER

One more losses that has major contribution to the losses in the inverter system is Switching losses of the switches used in the system. Three different methods are studied to reduce the losses and the one that is giving lower switching losses is selected [5].The switching loss for one cycle is assumed to be directly proportional to current. Therefore, the average switching loss per cycle can be calculated as

$$q_{sub}(\omega t) = \frac{K|i_1(\omega t)|}{T_S(\omega t)} \quad (4.3)$$

where K is a constant that depends upon DC voltage, i_1 is instantaneous current and Ts is switching period. Since, we are going to vary switching frequency in different methods, here Ts(ωt) is taken as a function. The switching losses can be given as

$$q_{sub}(\omega t) = \frac{KI_1\sqrt{2}\,|sin(\omega t - \varphi)|}{T_S(\omega t)} \tag{4.4}$$

Where, φ is the lagging angle of the grid current.

The average switching losses for a cycle can be derived as follows,

$$Q(T_S(\omega t)) = \frac{1}{\pi}\int_0^{\pi} q_{sub}(\omega t)d\omega t \tag{4.5}$$

$$= KI_1\sqrt{2}\int_0^{\pi}\frac{|sin(\omega t - \varphi)|}{T_S(\omega t)}d\omega t \tag{4.6}$$

A. Constant Switching Frequency Scheme

In this case we take constant switching frequency. Therefore Ts (ωt) remains constant. The switching losses graph would be a sinusoidal plot.

$$q_{sub}(T_S(\omega t)) = \frac{KI_1\sqrt{2}\,|sin(\omega t - \varphi)|}{T_S} \tag{4.7}$$

B. .Constant Ripple Scheme

In this case we take constant required rms current ripple. From that value peak to peak ripple is calculated,

$$\Delta I_{pk-pk} = 2\sqrt{3}\,\Delta I_{rms} \tag{4.8}$$

$$\Delta i_{pk-pk} = \frac{T_S V_{dc}}{2L}(1 - m_a\, sin\omega t).\, m_a sin\omega t \tag{4.9}$$

$$T_S(\omega t) = \frac{2\sqrt{3}\Delta I_{rms,req}L}{V_d\,(1-m_a|sinwt|)m_a|sin\omega t|}$$

$$q(\,T_S(\omega t)) = \frac{K\sqrt{2}I_1V_{dc}}{2\sqrt{3}\Delta I_{rms,req}}|\sin(\omega t - \varphi)|(1 - m_a|sinwt|)m_a|sin\omega t| \tag{4.10}$$

C. Optimal Switching Scheme

In this method, the value or function of T_s (ωt) is selected such that the switching losses are lower.

$$T_s(\omega t) = C' \sqrt[3]{\left(\frac{|\sin(\omega t-\varphi)|}{1-m_a|sinwt|)^2(m_a|sin\omega t|)^2}\right)} \quad (4.11)$$

$$C' = \frac{2\sqrt{3}\Delta I_{rms,req}L}{V_{dc}m_a \sqrt[3]{\sqrt{\frac{1}{\pi}}\int_0^{\pi}([sin\omega t-\varphi]^2\ (1-m_a sin\omega t)^2(sin\omega t)^2)d\omega t}} \quad (4.12)$$

$$q(\ T_S(\omega t)) = \frac{K\sqrt{2}I_1 \sqrt[\frac{2}{3}]{|\sin(\omega t-\varphi)|(1-m_a sin\omega t)m_a|sin\omega t|}}{C'} \quad (4.13)$$

4.4. HARMONICS

Current harmonics infused to the utility grid by a VSC might be diminished with a legitimately planned LCL filter as contrasted with a basic L or LC filter. Keeping in mind the end goal to exhibit this, the frequency response of these filters (LCL and L) are analyzed.

Accepting lossless parts and immaculate sinusoidal grid voltage at the fundamental frequency, the harmonic model of a LCL filter might be acquired. The grid voltage shows up as short circuit in this model for h≠1.All reactance are defined at fundamental frequency as [10]:

$$X = \omega L \quad (4.14)$$

$$X_g = \omega L_g \quad (4.15)$$

$$X_c = \frac{1}{\omega C} \quad (4.16)$$

Magnitude of the transfer function of LCL filter:

$$|H_{LCL}\ | = \frac{1}{h(X+X_g-\frac{XX_g}{X_c}h^2)} \quad (4.17)$$

The magnitude of the transfer function of a simple L filter from $i_g$to v is

$$|H_L| = \frac{1}{hX} \quad (4.18)$$

We normally keep the converter infused harmonic current as low as could be allowed alongside that the size and expense of the channel ought to likewise be minimized. The count of dominant frequency present alongside its current ripple in distinctive segments is likewise done. At long last, dissection of the impact of filter on closed loop execution of the general grid is likewise done. In this manner, notwithstanding better harmonic attenuation of a LCL

filter, an architect need to face muddled configuration issue in a LCL filter as contrasted with straightforward L filter.

4.5 SUMMARY

In this section, Comparison between unipolar and bipolar switching scheme with LCL Filter is carried out. The distinctive switching schemes for single phase full bridge inverter are contemplated and contrasted with get the exchanging plan which gives lesser exchanging losses. Current harmonics infused to the utility grid by a VSC could be lessened with a legitimately composed LCL filter as contrasted with a basic L or LC filter. The different switching schemes for single phase full bridge inverter are studied and compared to get the switching scheme which gives lesser switching losses.

CHAPTER 5

RESULTS AND DISCUSSION

Results and Discussion

RESULTS AND DISCUSSION

In order to plot all the graphs data has been taken from Table 1.1.

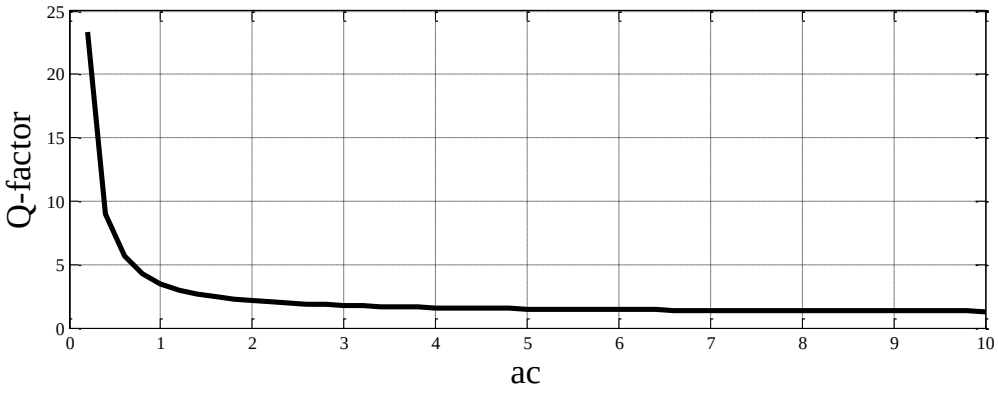

Fig 5.1.Q-Factor In Per Unit for the Damping Branch.

From the figure 5.1, we can see that there is no change in the Q of the frequency response if A_C is expanded past two. Along these lines, we are setting ac=1as the best decision, since it is essentially simple to design two capacitors of the same worth.

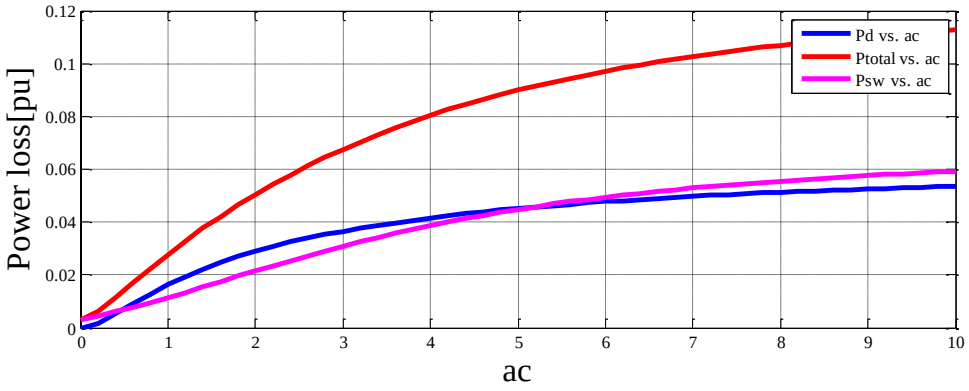

Fig 5.2. Power Dissipation in Per Unit for the Damping Branch

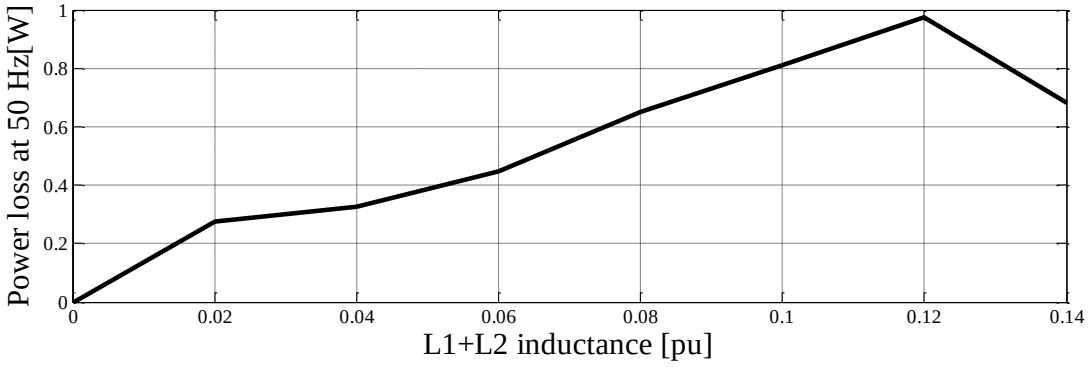

Fig 5.3. Core Loss Variation with the Inductance at Fundamental Frequency.

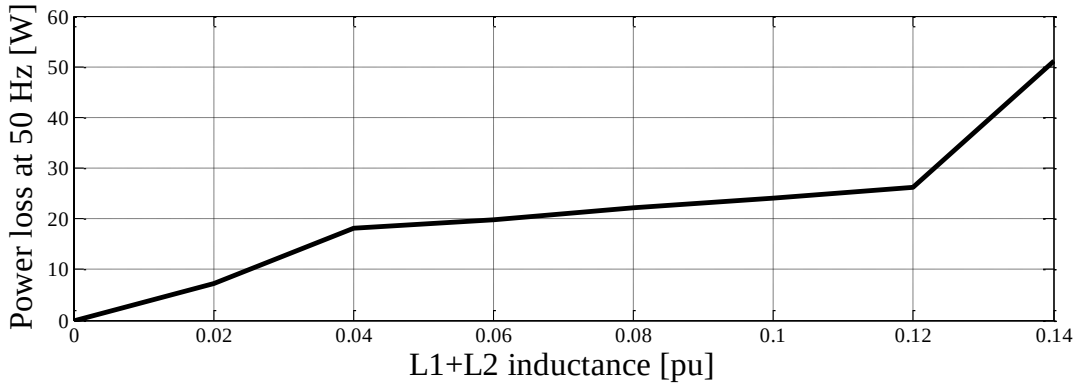

Fig 5.4. Copper Loss Variation with the Inductance at Fundamental Frequency.

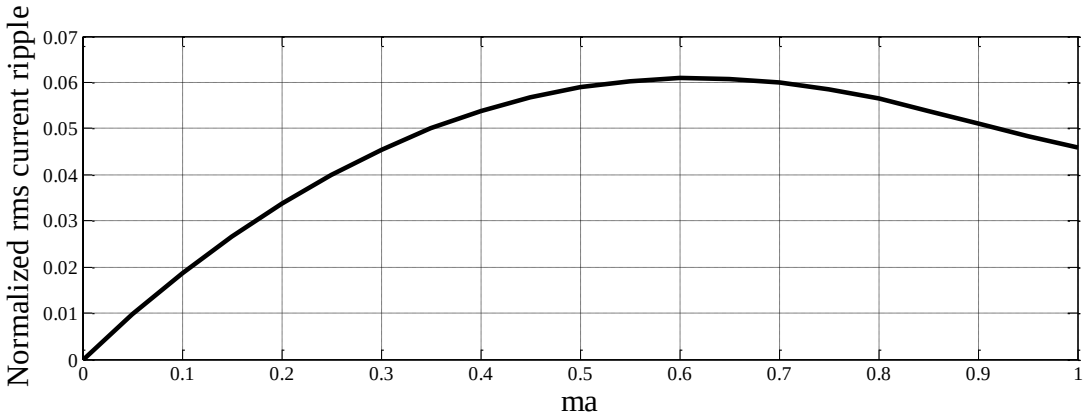

Fig 5.5. Normalized RMS Current Ripple Verses M_a

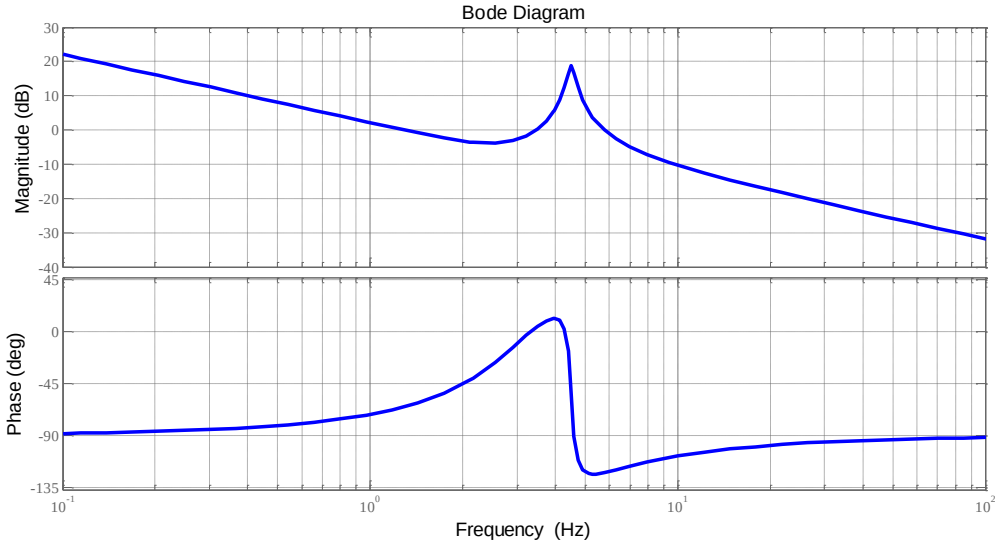

Fig 5.6. Control to Converter Current Transfer Function Bode Plot for Active Damping.

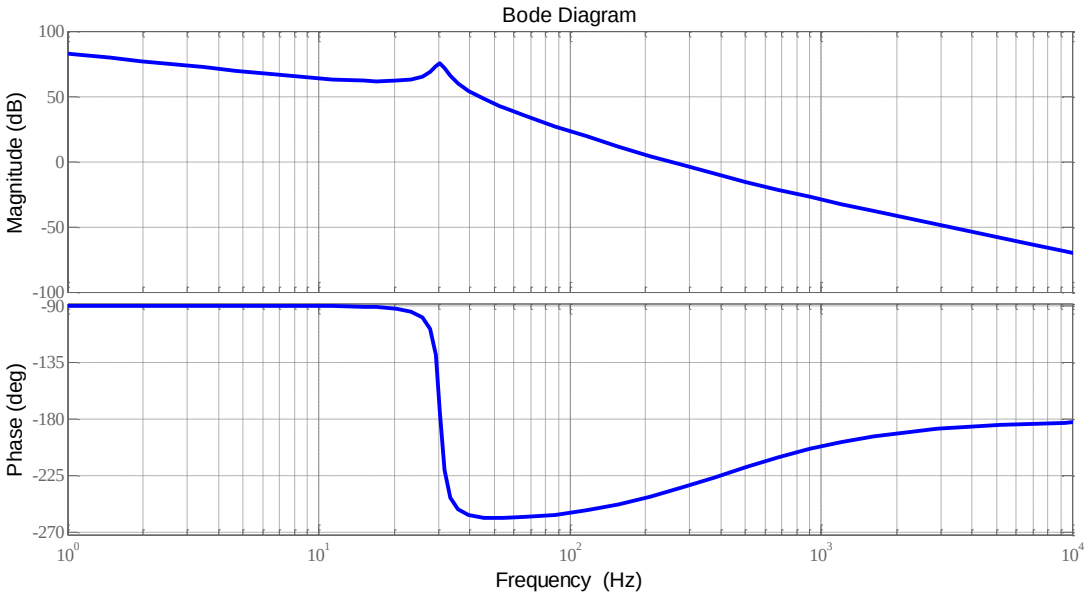

Fig 5.7. Control to Grid Current Transfer Function Bode Plot for Passive Damping.

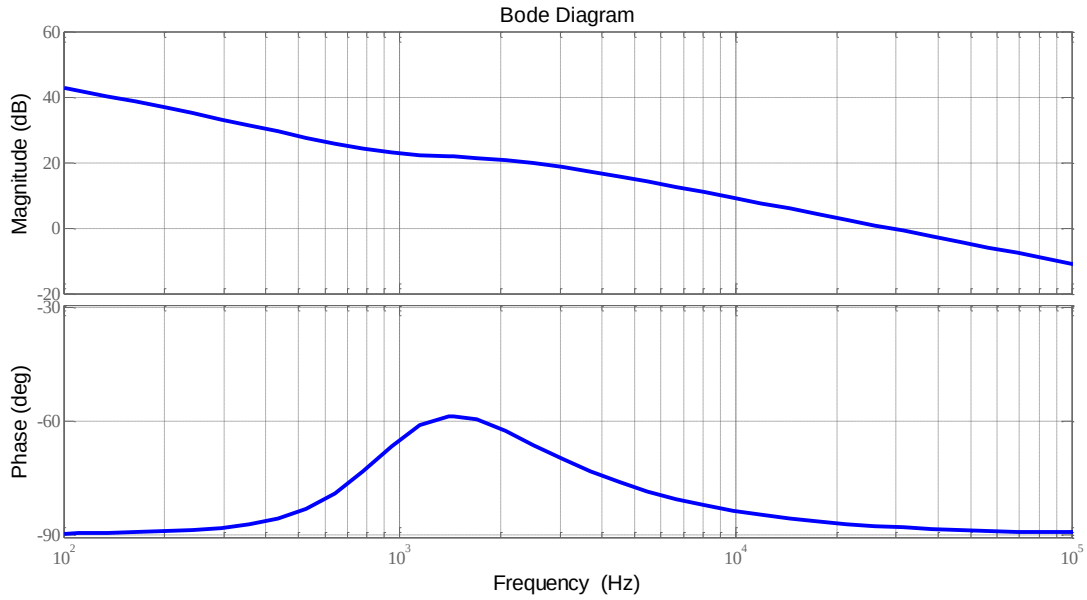

Fig 5.8. Control to Grid Current Transfer Function Bode Plot for Active Damping.

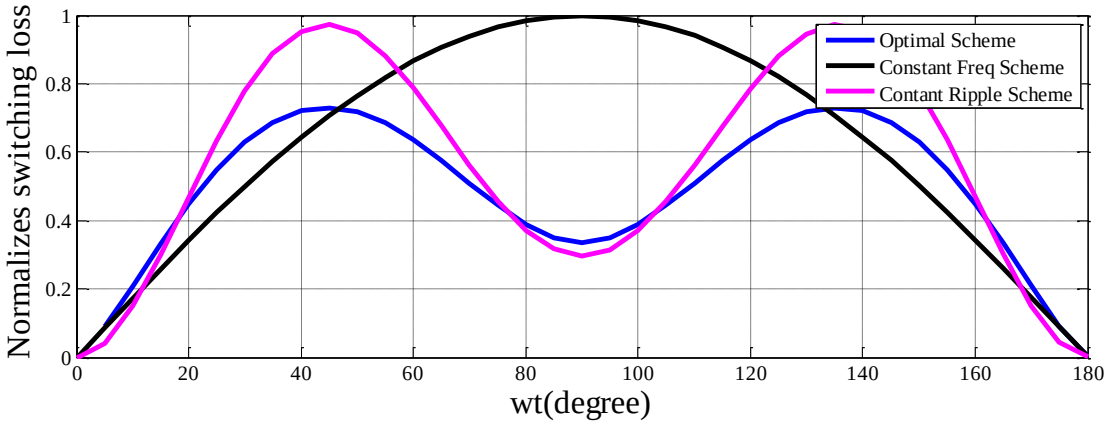

Fig 5.9. Time Variation of the Switching Frequency for M_a=0.95 and $\Phi = 0^0$.

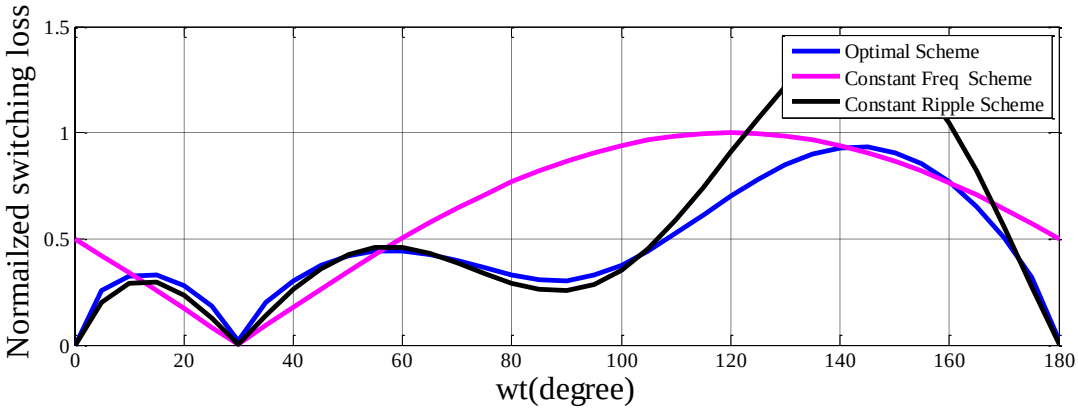

Fig 5.10 Time Variation of the Switching Frequency for M_a=0.95 and $\Phi=\Pi/6$.

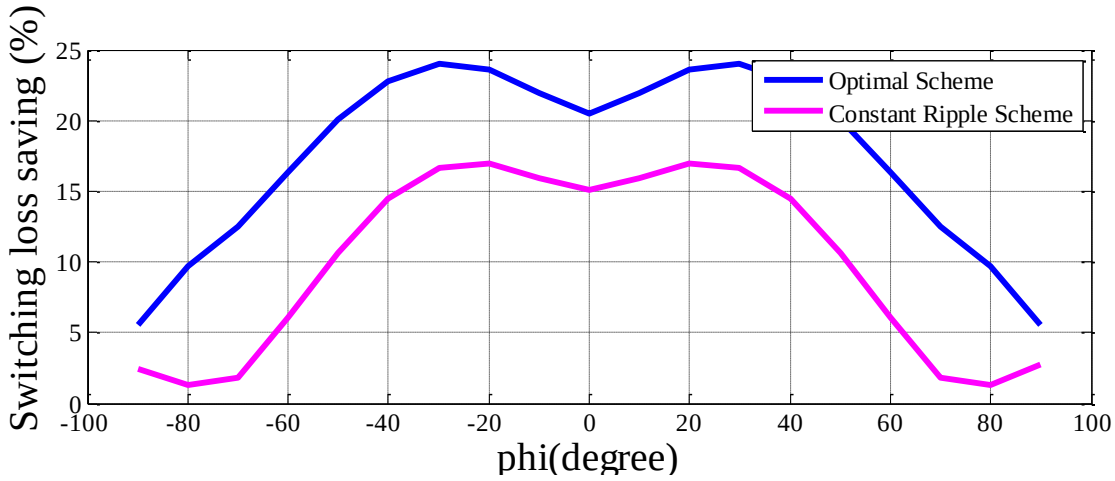

Fig 5.11. Switching Loss Saving Versus Φ For Ma=0.95.

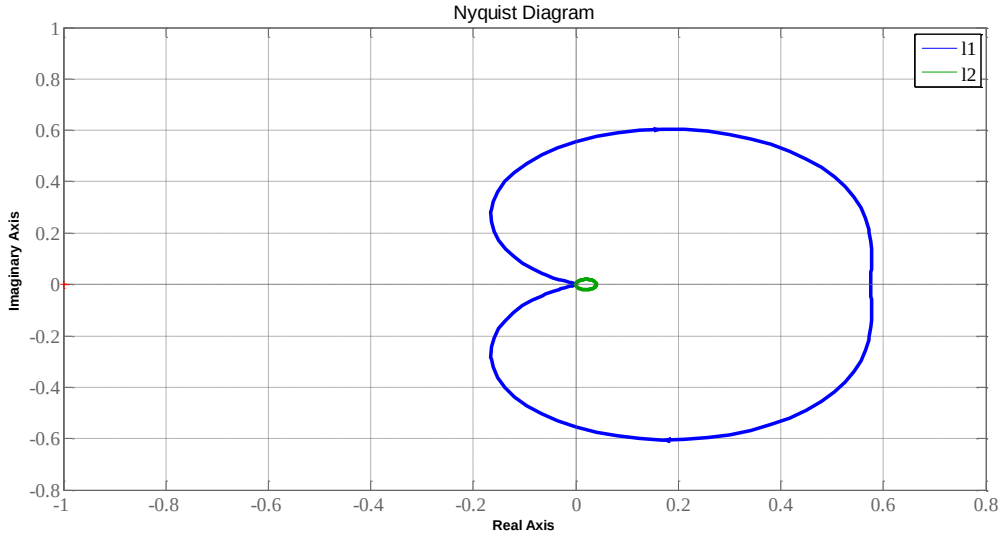

Fig 5.12. Nyquist Plots for the Eigenvalues of the Return-Ratio Matrix L_{dq} (S) Controlled with Converter-Side Current.

The dissection demonstrated that for gathering the same THD prerequisite with a given filter, the ideal exchanging plan spares up to 36.5% under "best-case" conditions contrasted with the fixed switching frequency scheme.

In Fig 5.12, the Nyquist diagram for $l_2(s)$is almost in the unit circle and does not intersect with the unit circle on the left plane of the complex plane. Whereas $l_1(s)$ presents large magnitude and does not encircle about (-1, j0), it intersects with the unit circle on the left plane of the complex plane and it influences the stability margin of the system.

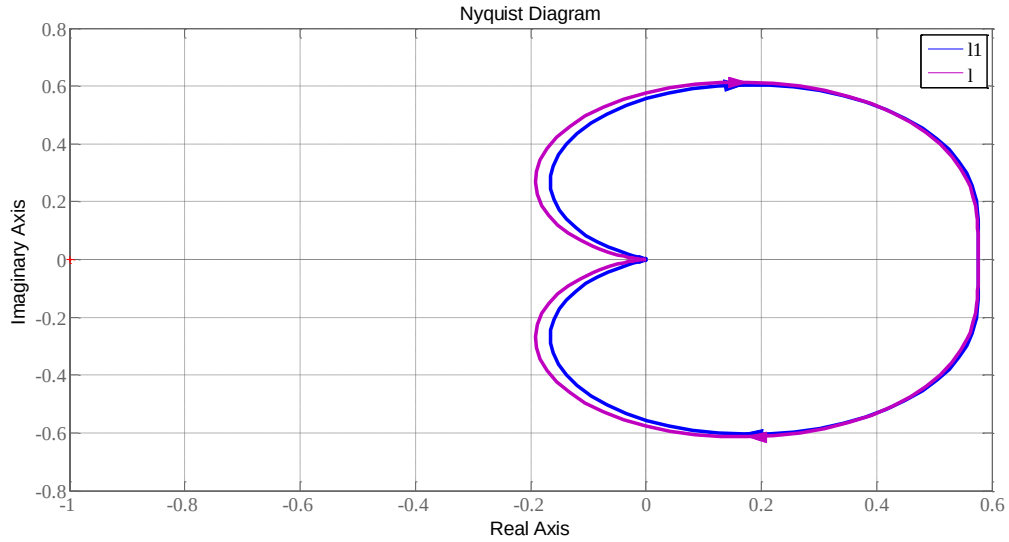

Fig 5.13 Nyquist plots for 1_1(s) and l (s).

Fig. 5.13 shows the Nyquist plots for $l_1(s)$ and $l_2(s)$. Therefore, the resistive component in the grid impedance is able to improve the stability margin of the grid-connected system. In order to guarantee a sufficient stability margin for the system, this paper considers extreme cases and $l(s)$ is utilized to analyze the stability margin of system.Therefore, the stability analysis of a grid-connected system with an LCL filter is converted into a study of the d-d channel output impedance $Z_{dd}(s)$ and the inductive component $Z_{Lg}(s)$ in the grid impedance. Further, it is indicated that the steadiness of the grid-connected system controlled with the converter-side current is completely dictated by the d-d channel output impedance of the grid connected inverter and the inductive part of the grid impedance, and the stability margin of the grid-connected inverter can be changed by regulating the LCL parameters.

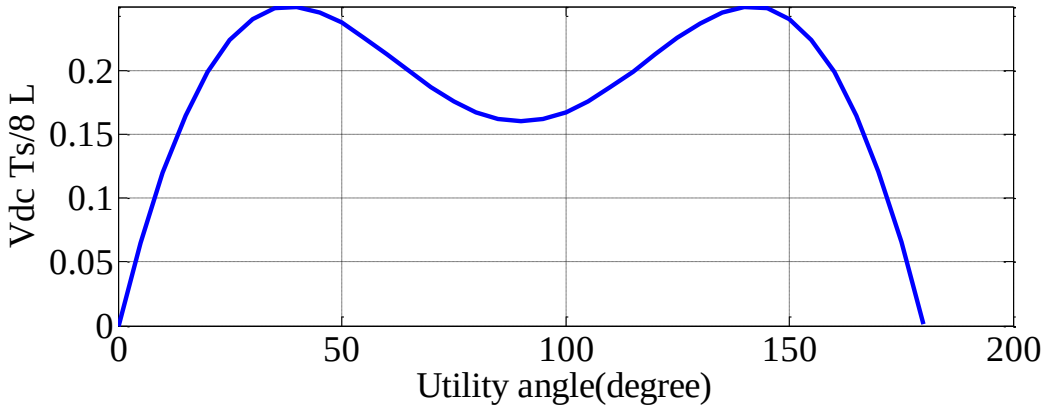

Fig 5.14 Magnitude distribution of Δi_{pk-pk} bipolar switching scheme for m_a=0.8

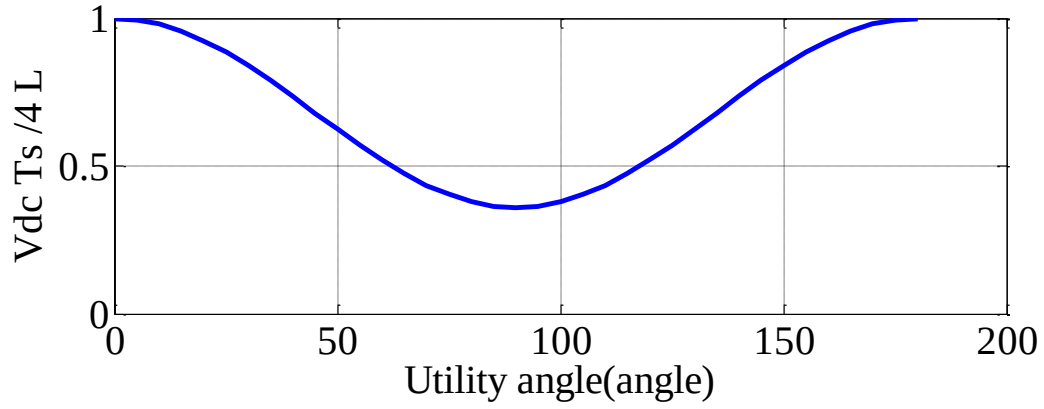

Fig 5.15. Magnitude distribution of Δi_{pk-pk} unipolar switching scheme for m_a = 0.8.

Fig 5.14 and Fig. 5.15 shows the size conveyance of Δi_{pk-pk} for both unipolar and bipolar switching schemes. Since, the voltage and current waveforms are half-wave symmetry, the circumstances throughout $\pi < \omega t < 2\pi$ rehashes same as that of throughout $0 < \omega t < \pi$.

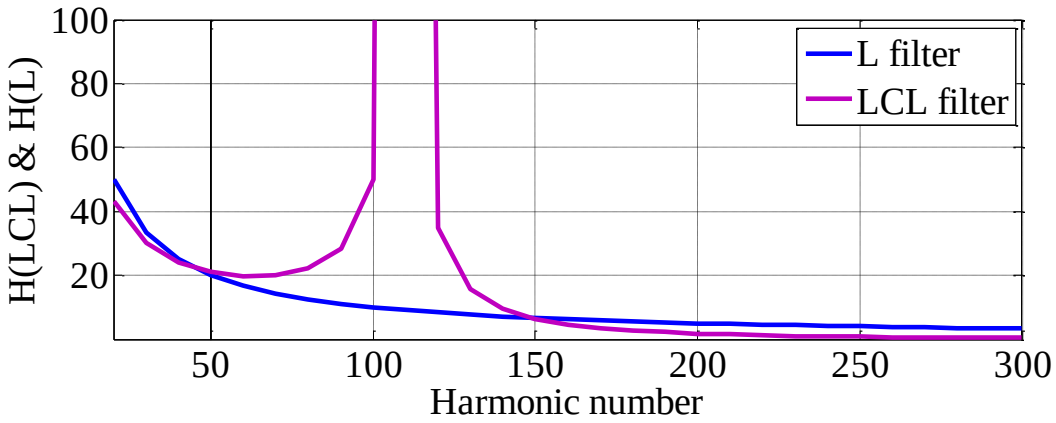

Fig 5.16 $|H_{LCL}|$ and $|H_L|$ versus Harmonic Number

Fig 5.16 shows the plot of $|H_{LCL}|$ and $|H_L|$ | versus harmonic order with X= 0. 001 for every unit, Xc=2 for every unit and Xg = X/5. It might be unmistakably seen that the LCL filter has better constriction especially at frequencies over the 50th harmonic.

CHAPTER 6

CONCLUSION

Conclusion

Scope of Future Work

6.1. CONCLUSION

Optimal LCL filter design along with switching loss reduction is presented. Hence, the optimal filter is designed considering THD% and ripple factor. And for that value of inductor different switching losses are studied. The analysis showed that for meeting the same THD requirement with a given filter, the optimal switching scheme saves up to 36.5% under “best-case” conditions compared to the fixed switching frequency scheme. Thus, using this scheme can reduce the size of the heat sink or, for an existing heat sink design, reduce the temperature of the switches and possibly extend the inverter life. The total LCL filter loss per phase was plotted.

These loss curves were used to find the most efficient LCL filter design. A frequency-domain analysis to design the control systems, system stability and the control scheme of the grid current based on the averaged small-signal model is studied. The resistive component in the grid impedance is able to improve the stability margin of the grid-connected system.

6.2. SCOPE OF FUTURE WORK

The work done so far considers only few aspects. Some aspects of stability like dynamic stability have not been taken into consideration and also power quality issues.

REFERENCES

[1] Channegowda, P.; John, V.; , "Filter Optimization for Grid Interactive Voltage Source Inverters," Industrial Electronics, IEEE Transactions on, vol.57, no.12, pp.4106-4114, Dec. 2010.

[2] Jiri Lettl, Jan Bauer, and Libor Linhar; "Comparison of Different Filter Types for Grid Connected Inverter", PIERS Proceedings, Marrakesh, MOROCCO, March 20-23, 2011.

[3] Yibin Tong, Fen Tang, Yao Chen, Fei Zhou, and Xinmin Jin; "Design Algorithm of Grid-side LCL-filter for Three-phase Voltage Source PWM Rectifier", J. A. Ferreira, "Improved analytical modelling of conductive losses in magnetic components,"IEEE Trans. Power Electron., vol. 9, no. 1, pp. 127–131, Jan. 1994.

[4] M. Bartoli, A. Reatti, and M. K. Kazimierczuk, "Modelling winding losses in high frequency power inductors," J. Circuits, Syst. Comput.,vol.5,no. 4, pp. 607–626, Dec. 1995.

[5] Xiaolin Mao; Ayyanar, R.; Krishnamurthy, H.K.; , "Optimal Variable Switching Frequency Scheme for Reducing Switching Loss in Single Phase Inverters Based on Time-Domain Ripple Analysis," Power Electronics, IEEE Transactions on , vol.24, no.4, pp.991-1001, April 2009.

[6] Erickson. RW, fundamental of Power Electronics; Norwell MA, Kluwer, 1997.S

[7] Xiao-Qiang Li, Xiao-Jie Wu, Yi-Wen Geng, and Qi Zhang; "Stability Analysis of Grid-Connected Inverters with an LCL Filter Considering Grid Impedance", Journal of Power Electronics, Vol. 13, No. 5, September 2013.

[8] Hyosung Kim, Kyoung-Hwan Kim, "Filter design for grid connected PV inverters", Proc. of IEEE International on Sustainable Energy Technologies, ICSET200), pp.1070-1075, 2008.

[9] Debati Marandi, Tontepu Naga Sowmya, and B Chitti Babu Member, IEEE; , "Comparative Study between Unipolar and Bipolar Switching Scheme with LCL Filter for Single-Phase Grid Connected Inverter System", 2012 IEEE Students' Conference on Electrical, Electronics and Computer Science.

[10] Hamid R. Karshenas, Hadi Saghafi; , “Basic Criteria in Designing LCL Filters for Grid

[11] Connected Converters Basic Criteria in Designing LCL Filters for Grid Connected Converters” , IEEE ISIE 2006, July 9-12, 2006, Montreal, Quebec, Canada.

[12] Karshenas, H.R.; Saghafi, H., "Performance Investigation of LCL Filters in Grid Connected Converters," *Transmission & Distribution Conference and Exposition: Latin America, 2006. TDC '06. IEEE/PES* , vol., no., pp.1,6, 15-18 Aug. 2006

[13] P. Daly and J. Morrison," Understanding the Potential Benefits of Distributed Generation on Power Delivery," IEEE Rural Electric Power Conference, 2001

[14] J. F. Manwell, et al, Wind Energy Explained, John Wiley & Sons Ltd., 2002.

[15] M. Liserre, F. Blaabjerg, and S. Hansen "Design and Control of an LCL-Filter-Based Three-Phase Active Rectifier," IEEE Trans. Industry Applications, vol. 41, no. 5, pp. 1281-1291, September/October 2005.

[16] M. Lindgren and J. Svensson," Control of a Voltage-source Converter Connected to the Grid through an LCL-filter-Application to Active Filtering," in Proc. PESC'98, vol. 1, 1998, pp. 229-235.

[17] M. Lindgren and J. Svensson," Current Control of Voltage Source Converters connected to the grid through an LCL-filter," in Proc. PESC'04, vol. 1, 2004, pp. 125-132.